AGU PUBLICATIONS

Paleoceanography

RESEARCH ARTICLE
10.1002/2013PA002579

Key Points:
- Winter monsoon strength influences productivity and SST off Pakistan
- Late Holocene NE monsoon intensity is anticorrelated with the Asian SW monsoon
- The winter monsoon record is in phase with Northern Hemisphere climate periods

Supporting Information:
- Readme
- Figure S1
- Figure S2
- Figure S3
- Figure S4
- Text S1

Correspondence to:
A. Böll,
anna.boell@zmaw.de

Citation:
Böll, A., A. Lückge, P. Munz, S. Forke, H. Schulz, V. Ramaswamy, T. Rixen, B. Gaye, and K.-C. Emeis (2014), Late Holocene primary productivity and sea surface temperature variations in the northeastern Arabian Sea: Implications for winter monsoon variability, *Paleoceanography*, *29*, 778–794, doi:10.1002/2013PA002579.

Received 7 NOV 2013
Accepted 15 JUL 2014
Accepted article online 18 JUL 2014
Published online 7 AUG 2014

Late Holocene primary productivity and sea surface temperature variations in the northeastern Arabian Sea: Implications for winter monsoon variability

Anna Böll[1], Andreas Lückge[2], Philipp Munz[3], Sven Forke[4], Hartmut Schulz[3], V. Ramaswamy[5], Tim Rixen[1,4], Birgit Gaye[1], and Kay-Christian Emeis[1,6]

[1]Institute of Biogeochemistry and Marine Chemistry, University of Hamburg, Hamburg, Germany, [2]Bundesanstalt für Geowissenschaften und Rohstoffe, Hannover, Germany, [3]Department of Geosciences, University of Tübingen, Tübingen, Germany, [4]Leibniz Center for Tropical Marine Ecology, Bremen, Germany, [5]National Institute of Oceanography, Goa, India, [6]Institute of Coastal Research, Helmholtz Center Geesthacht, Geesthacht, Germany

Abstract Variability in the oceanic environment of the Arabian Sea region is strongly influenced by the seasonal monsoon cycle of alternating wind directions. Prominent and well studied is the summer monsoon, but much less is known about late Holocene changes in winter monsoon strength with winds from the northeast that drive convective mixing and high surface ocean productivity in the northeastern Arabian Sea. To establish a high-resolution record of winter monsoon variability for the late Holocene, we analyzed alkenone-derived sea surface temperature (SST) variations and proxies of primary productivity (organic carbon and $\delta^{15}N$) in a well-laminated sediment core from the Pakistan continental margin. Weak winter monsoon intensities off Pakistan are indicated from 400 B.C. to 250 A.D. by reduced productivity and relatively high SST. At about 250 A.D., the intensity of the winter monsoon increased off Pakistan as indicated by a trend to lower SST. We infer that monsoon conditions were relatively unstable from ~500 to 1300 A.D., because primary production and SST were highly variable. Declining SST and elevated biological production from 1400 to 1900 A.D. suggest invigorated convective winter mixing by strengthening winter monsoon circulation, most likely a regional expression of colder climate conditions during the Little Ice Age on the Northern Hemisphere. The comparison of winter monsoon intensity with records of summer monsoon intensity suggests that an inverse relationship between summer and winter monsoon strength exists in the Asian monsoon system during the late Holocene, effected by shifts in the Intertropical Convergence Zone.

1. Introduction

The Asian monsoon system is one of the most important components of global climate. Although variations in the Asian monsoon have a great impact on climatological and biogeochemical processes in the ocean as well as on land, there are yet few high-resolution studies recording monsoon variability during the last 2000 years. One opportunity to establish such high-resolution records of late Holocene climate change comes from laminated sediments deposited on the Makran continental margin in the northeastern Arabian Sea [*von Rad et al.*, 1999; *Doose-Rolinski et al.*, 2001; *Lückge et al.*, 2001].

Primary productivity in the Arabian Sea is high and is tightly linked to the seasonal dynamics of the Asian monsoon system. Forced by reversing atmospheric pressure gradients between central Asia and the southern Indian Ocean and accompanied by shifts in the Intertropical Convergence Zone (ITCZ) [*Clemens et al.*, 1991], low-level winds reverse direction in the course of the year. Strong southwesterly winds during the summer months caused by differential land-ocean heating in spring [*Hastenrath and Lamb*, 1979] induce clockwise surface water circulation in the Arabian Sea. As a consequence, upwelling of nutrient-rich waters along the coast off Somalia, Oman, and southwest India supports high biological productivity during the months June to September [*Nair et al.*, 1989; *Haake et al.*, 1993; *Rixen et al.*, 1996]. A secondary primary productivity peak in the northern basin is initiated when the wind direction reverses due to faster cooling of the continent in fall [*Rixen et al.*, 2005]. Prevailing moderate and dry northeasterly winds in winter drive a counterclockwise surface circulation and cool Arabian Sea surface waters [*Wyrtki*, 1973], thereby initiating convective winter mixing that provides nutrients for seasonally and regionally enhanced biological productivity [*Banse and McClain*, 1986; *Madhupratap et al.*, 1996].

©2014. American Geophysical Union. All Rights Reserved.

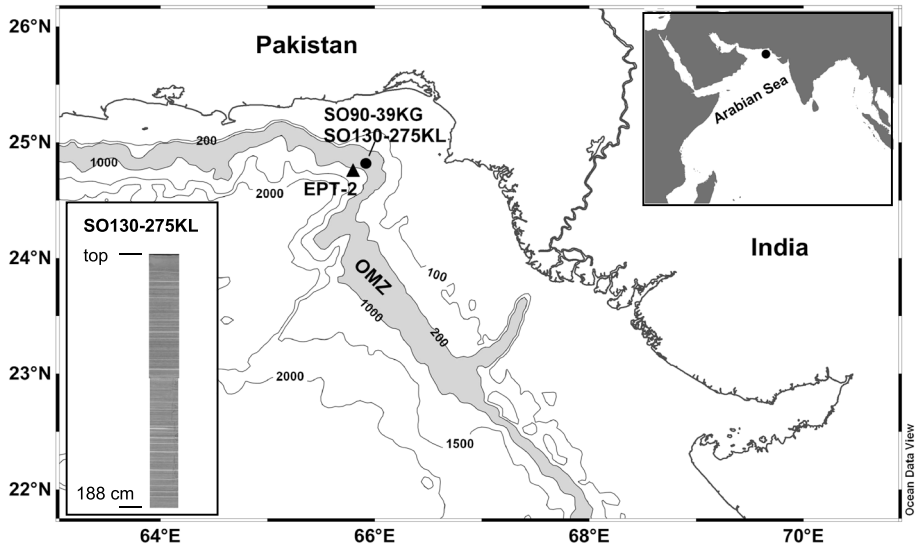

Figure 1. Study area in the northeastern Arabian Sea off Pakistan with core locations 275KL and 39KG and sediment trap station EPT-2. The shaded area indicates OMZ impinging on the continental slope. Bathymetry is shown in meters. Inset: vertical profile of core 275KL showing varve-like lamination. This map is produced by using Ocean Data View [*Schlitzer*, 2013].

Whereas most sediment trap studies in the central Arabian Sea indeed indicate highest biological productivity during the summer monsoon [*Broerse et al.*, 2000; *Prahl et al.*, 2000; *Wakeham et al.*, 2002]; highest particle fluxes in the northeastern Arabian Sea are observed during the winter monsoon season [*Andruleit et al.*, 2000; *Lückge et al.*, 2002; *Schulz et al.*, 2002; *Rixen et al.*, 2005] and are associated with sea surface cooling down to about 23°C. Hence, periods of low sea surface temperatures (SSTs) in the northeastern Arabian Sea are linked to the cool northeast monsoonal winds during winter.

We know today that monsoon activity varied not only on Milankovitch time scales but also during the late Holocene, as evident in Arabian Sea sediments [*von Rad et al.*, 1999; *Lückge et al.*, 2001; *Anderson et al.*, 2002, 2010; *Gupta et al.*, 2003, 2011; *Agnihotri et al.*, 2008; *Chauhan et al.*, 2010] and in various cave records from Oman [*Burns et al.*, 2002; *Fleitmann et al.*, 2004], Yemen [*Van Rampelbergh et al.*, 2013], India [*Sinha et al.*, 2007, 2011; *Berkelhammer et al.*, 2010], and China [*Zhang et al.*, 2008]. Similarly, primary productivity in the Arabian Sea was not uniform on time scales of a few hundred thousand years but tracked monsoon variations caused by glacial/interglacial cycles [*Rostek et al.*, 1997; *Schulz et al.*, 1998; *Schulte et al.*, 1999; *Schulte and Müller*, 2001]. Although some knowledge exists about summer monsoon-related changes in primary productivity over the last 2000 years from the Oman Margin [*Anderson et al.*, 2002, 2010; *Gupta et al.*, 2003] and the southwestern coast off India [*Agnihotri et al.*, 2008], paleoceanographic responses to late Holocene winter monsoon variability in the northeastern Arabian Sea are unknown.

Here we report a high-resolution record of winter monsoon variability for the late Holocene discerned from changes in primary productivity and sea surface temperature for the mainly winter monsoon-dominated northeastern Arabian Sea. We analyzed a 188 cm long section of a well-laminated sediment core from the Pakistan Margin (Figure 1) for bulk components (organic carbon, carbonate, and opal), stable nitrogen isotopes, and alkenone unsaturation ratios to reconstruct the productivity and monsoon variability throughout the last 2400 years. A key proxy for the winter monsoon intensity is the alkenone-derived SST estimate, which we validate by analyzing the seasonality of the alkenone-based SST signal at eastern PAKOMIN sediment trap station (EPT-2) close to our core location. Our detailed objectives are to (1) examine the relationship between SST and alkenone unsaturation ratios in sediment trap material for the northeastern Arabian Sea, (2) reconstruct late Holocene (winter monsoon-dominated) SST and paleoproductivity changes for the northeastern Arabian Sea, (3) compare the winter monsoon-dominated record with records of summer monsoon variability to learn about the dynamics of the monsoon low-level wind system,

©2014. American Geophysical Union. All Rights Reserved.

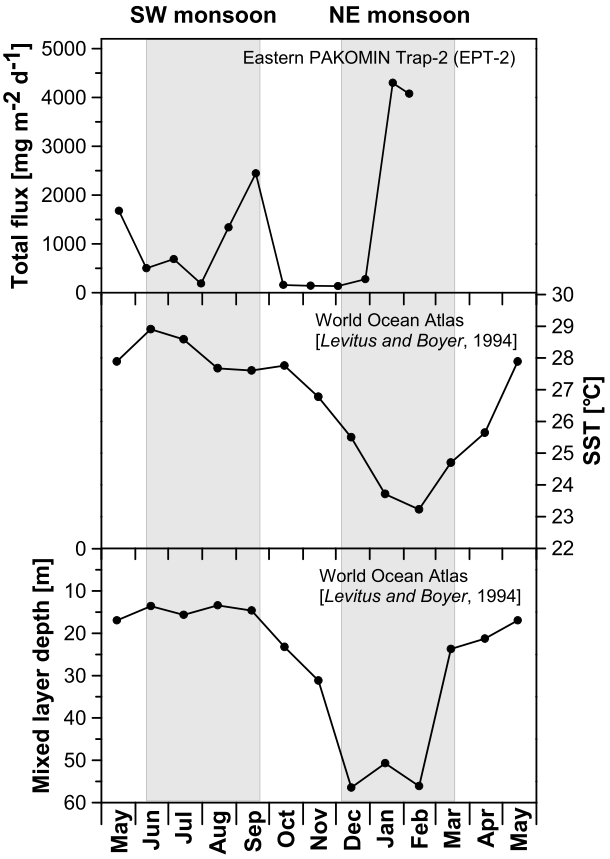

Figure 2. Annual variability of mixed layer depth and SST for site 275KL extracted from the World Ocean Atlas [*Levitus and Boyer*, 1994] and total particle flux measured in sediment trap EPT-2 after *Andruleit et al.* [2000]. Increased particle fluxes occur during the NE monsoon season when strong convective winter mixing deepens the mixed layer and SST decreases.

and (4) examine possible links in the regional wind and surface ocean system to Northern Hemisphere climate change in historical time.

2. Study Area

Unlike offshore the coast of Somalia, Oman, and southeast India, upwelling does not occur during the southwest (SW) monsoon season on the Pakistan Margin, so that SSTs are warm during summer (27.8 to 29.3°C). In the northeastern Arabian Sea, high productivity during the SW monsoon in summer is partly supported by the lateral advection of nutrient-rich surface waters from the upwelling area off Oman [*Schulz et al.*, 1996]. Cool winter SSTs (~23°C) during the northeast (NE) monsoon season are accompanied by a deepening of the mixed layer through convective mixing (Figure 2) that stimulates a second peak in primary production [*Banse and McClain*, 1986; *Madhupratap et al.*, 1996]. During this season, reduced solar insolation together with enhanced evaporation lead to density increase of surface waters and convective deepening of the mixed layer over the Pakistan Margin. Concentrations of nitrate and chlorophyll *a* and primary production in the surface layer here correlate with mixed layer depth and wind speeds [*Madhupratap et al.*, 1996; *Prasanna Kumar and Prasad*, 1996; *Prasanna Kumar et al.*, 2001]. Increased particle fluxes during the months of January and February indicate even higher production during the NE monsoon season than during the SW monsoon season over the Pakistan Margin [*Andruleit et al.*, 2000; *Schulz et al.*, 2002; see Figure 2].

In the northern Arabian Sea, a stable midwater oxygen minimum zone (OMZ) between 200 and 1200 m water depth is maintained by high organic matter fluxes and subsequent oxygen consumption during mineralization of organic matter, combined with reduced vertical mixing caused by the input of warm, saline water masses from the Persian Gulf and the Red Sea to intermediate water depths [*Olson et al.*, 1993; *Schulz et al.*, 1996]. High organic matter fluxes from the euphotic zone raise rates of denitrification in the OMZ, which in turn raise the $\delta^{15}N$ values of thermocline nitrate mixed into the surface layer and assimilated by phytoplankton. Intensification of the OMZ thus results in high sedimentary $\delta^{15}N$ values upon burial of particulate N, whereas weakening of the OMZ and reduced denitrification intensity lead to low sedimentary $\delta^{15}N$ values [e.g., *Altabet et al.*, 1995; *Naqvi et al.*, 1998; *Suthhof et al.*, 2001; *Gaye-Haake et al.*, 2005].

Sediments deposited within the OMZ depth interval on the Pakistan Margin are laminated with alternating dark and light sediment layers and record high input of lithogenic material originating from dust storms and/or river runoff [*von Rad et al.*, 1995, 1999; *Schulz et al.*, 1996]. *Lückge et al.* [2002] showed that dark laminae are deposited over large parts of the year and reflect primary production of marine organic matter, whereas light-colored laminae contain almost exclusively land-derived materials which are deposited in the winter season during short-term heavy rainfall events.

©2014. American Geophysical Union. All Rights Reserved.

3. Methods

3.1. Sample Collection and Stratigraphy

In this study we investigated piston core 275KL and box core 39KG, both located within the center of the OMZ off the Pakistan coast (Figure 1). The box core 39KG (24°50.01′N, 65°55.01′E; 695 m water depth) was collected in 1993 during SONNE cruise 90, and results were published by *von Rad et al.* [1999], *Doose-Rolinski et al.* [2001], and *Lückge et al.* [2001]. The piston core 275KL was retrieved from the same position in 1998 during SONNE cruise 130 (24°49.31′N, 65°54.60′E; 782 m water depth). We studied the top 188 cm interval of core 275KL and the top 15 cm of core 39KG, which together yield a continuous record of environmental conditions on the Pakistan Margin over the last 2400 years. Core 275KL was continuously sampled in 0.5 cm intervals (sample resolution of 5 to 80 years) for bulk analysis (organic carbon and carbonate), and every third or fourth sample (of this sample series) was analyzed for opal concentrations and stable nitrogen isotope measurements. Alkenones were measured at continuous 2 cm intervals in core 275KL. In core 39KG, all parameters were analyzed on 1 cm intervals (6 to 8 year resolution). All samples were freeze dried and homogenized with mortar and pestle prior to chemical treatment and analyses.

In addition to seasonal varves, core 275KL exhibits reddish brown silt turbidites up to 9 cm thick and light gray short event deposits (>1 mm thick) consisting of allochthonous lithotypes interpreted as "plume deposits" by episodically heavy river floods that transport mud suspensions across the narrow shelf onto the steep upper slope [*Lückge et al.*, 2002; *von Rad et al.*, 2002a]. Sediments containing these event deposits or turbidites were excluded from our sample set.

Varves, turbidites, and event layers in our core are equivalent to the lithostratigraphy observed in core 56KA from the same position. Core 56KA has been dated by *von Rad et al.* [1999] by varve counting and several conventional and accelerator mass spectrometry ^{14}C datings. Our age model is based on the visual correlation of event deposit layers from both cores as stratigraphic tie points and interpolation between these tie points (Figure S1 in the supporting information).

We also analyzed alkenones and calculated alkenone fluxes as well as the $U^{K'}_{37}$ index of samples from the eastern PAKOMIN sediment trap mooring station (EPT-2; 24°45.6′N, 65°48.7′E; 590 m water depth) to ascertain the validity of sea surface temperatures estimated in sediment core samples. The EPT-2 trap was deployed from May 1995 to February 1996 and was previously studied by *Andruleit et al.* [2000] and *Schulz et al.* [2002].

3.2. Bulk Components (Organic Carbon, Carbonate, and Opal)

Total carbon was analyzed on a Carlo Erba 1500 elemental analyzer (Milan, Italy) with a precision of 0.2%. Total organic carbon (TOC) was measured with the same instrument after samples were treated with 1 *M* hydrochloric acid (HCl) to remove inorganic carbon. Analytical precision for organic carbon was 0.02%. Carbonate carbon was calculated as the difference between total carbon and organic carbon.

Biogenic opal was determined by wet alkaline extraction of biogenic silica (BSi) using a variation of the DeMaster method [*DeMaster*, 1981]. About 30 g sediment per sample was digested in 40 mL of 1% sodium carbonate solution (Na_2CO_3) in a shaking bath at 85°C. After 3 h, the supernatant was withdrawn and neutralized in 0.021 *M* HCl. The concentration of dissolved silica in the subsamples was determined photometrically. Biogenic opal was calculated by multiplying the BSi concentrations with a factor of 2.4. The mean standard deviation based on duplicate measurements of samples is 0.17%. To ensure that BSi is not overestimated by mineral dissolution at low BSi concentrations, we analyzed representative samples after 3, 4, and 5 h and used a slope correction for the determination of BSi concentrations [*Conley*, 1998]. The amount of BSi was then estimated from the intercept of the line through the time course aliquots [*DeMaster*, 1981]. Results of slope-corrected opal estimates showed that our method slightly overestimated opal concentrations by a mean of 0.13%. All bulk components are presented as weight percent.

Mass accumulation rates of organic carbon were calculated by multiplying the dry bulk densities of the sediments (measured at the Department of Geosciences, University of Tübingen) with calculated sedimentation rates and the weight fraction of organic carbon.

©2014. American Geophysical Union. All Rights Reserved.

3.3. X-ray Elemental Analysis

X-ray fluorescence (XRF) core scanner data were collected by XRF core scanner I at MARUM–Center for Marine Environmental Sciences (University of Bremen) using a Kevex Psi Peltier cooled silicon detector and a Kevex X-ray tube with the target material molybdenum (Mo). Counts were acquired directly at the split core surface of the archive half every 2 mm downcore over an area of 0.2 cm^2 with an instrument slit size of 2 mm using a generator setting of 20 kV, 0.087 mA, and a sampling time of 30 s. The split core surface was covered with a polypropylene foil to avoid contamination of the XRF measurement unit and desiccation of the sediment.

3.4. Nitrogen Stable Isotope Ratios

The ratio of the two stable isotopes of nitrogen ($^{15}N/^{14}N$) is expressed as $\delta^{15}N$, which is given as the per mil deviation from the N isotope composition of atmospheric N_2 ($\delta^{15}N = 0‰$): $\delta^{15}N = ((R_{Sample} - R_{Standard})/R_{Standard}) \times 1000$, where R_{Sample} is the $^{15}N/^{14}N$ ratio of the sample and $R_{Standard}$ is the $^{15}N/^{14}N$ ratio of atmospheric N_2. The $\delta^{15}N$ values were determined using a Finnigan MAT 252 gas isotope mass spectrometer after high-temperature flash combustion in a Carlo Erba NA-2500 elemental analyzer at 1100°C. Pure tank N_2 calibrated against the International Atomic Energy Agency reference standards IAEA-N-1 and IAEA-N-2, which were, in addition to an internal sediment standard, also used as working standards. Analytical precision based on replicate measurements of a reference standard was better than 0.1‰. Duplicate measurements of samples resulted in a mean standard deviation of 0.07‰.

3.5. Alkenones

Freeze-dried and homogenized sediment samples (1 to 3 g) were extracted twice for 5 min with methylene chloride (DCM) using an accelerated solvent extractor (Dionex; temperature 75°C, pressure 70 bar). Directly after extraction, a known amount of internal standard (14-heptacosanone) was added to the extracts. The extracts were then rotary evaporated until near dryness and saponified with 5% methanolic potassium hydroxide (KOH) solution overnight. The KOH solution was dried under a nitrogen flow, dissolved in DCM, and cleaned over a silica gel column using DCM as eluent. The clean fraction containing the alkenones was dried under N_2 and taken up in n-hexane (50–150 μL) prior to analysis. Alkenones were analyzed by gas chromatography on an Agilent 6850 gas chromatograph (GC) equipped with a split-splitless inlet system and flame ionization detector (310°C). Separation was achieved on a silica column (30 m × 0.1 μm film thickness × 0.32 mm ID; Optima1; Macherey–Nagel) using hydrogen as carrier gas (1 mL min^{-1}). The GC oven maintained 50°C for the first minute and was then programmed from 50° to 230°C at 20°C min^{-1}, from 230° to 260°C at 4.5°C min^{-1}, and from 260° to 320°C at 1.5°C min^{-1} followed by an isothermal period of 15 min. $C_{37:2}$ and $C_{37:3}$ alkenones were identified by comparing peak retention times between sediment samples and a working sediment standard. Quantification of alkenones was achieved by integrating the peak areas of the C_{37} alkenones and that of the internal standard (14-heptacosanone). Since both the C_{37} alkenones and the internal standard are very similar in structure, no different response factors between the C_{27} ketone and the C_{37} alkenones are assumed. Alkenones were translated into sea surface temperature using the core top calibration for the Indian Ocean from *Sonzogni et al.* [1997a]: $SST = (U^{K'}_{37} - 0.043)/0.033$ with $U^{K'}_{37} = C_{37:2}/(C_{32:2} + C_{37:3})$. Replicate extraction and measurement of a working sediment standard resulted in a mean standard deviation of estimated SST of 0.5°C.

4. Results

4.1. Alkenone Fluxes and $U^{K'}_{37}$ in Sediment Traps

Alkenone fluxes in EPT-2 between May 1995 and February 1996 ranged from 0.15 μg m^{-2} d^{-1} to 1.21 μg m^{-2} d^{-1} (see Figure 3a). Peak fluxes occurred in May 1995 (1.21 μg m^{-2} d^{-1}) and during the late NE monsoon in January 1996 (0.92 μg m^{-2} d^{-1}) and February 1996 (0.94 μg m^{-2} d^{-1}). Alkenone fluxes for the months September and October could not be determined due to low amounts of sample material. Alkenone fluxes on the Pakistan continental margin track coccolith fluxes during the seasonal cycle [*Andruleit et al.*, 2000] with maxima at the onset of the summer and of the winter monsoon. This underscores a strong link between primary and alkenone production. Alkenone (C_{37}) fluxes on the Pakistan Margin match those from the Oman Margin [*Wakeham et al.*, 2002] but are slightly lower than the total

©2014. American Geophysical Union. All Rights Reserved.

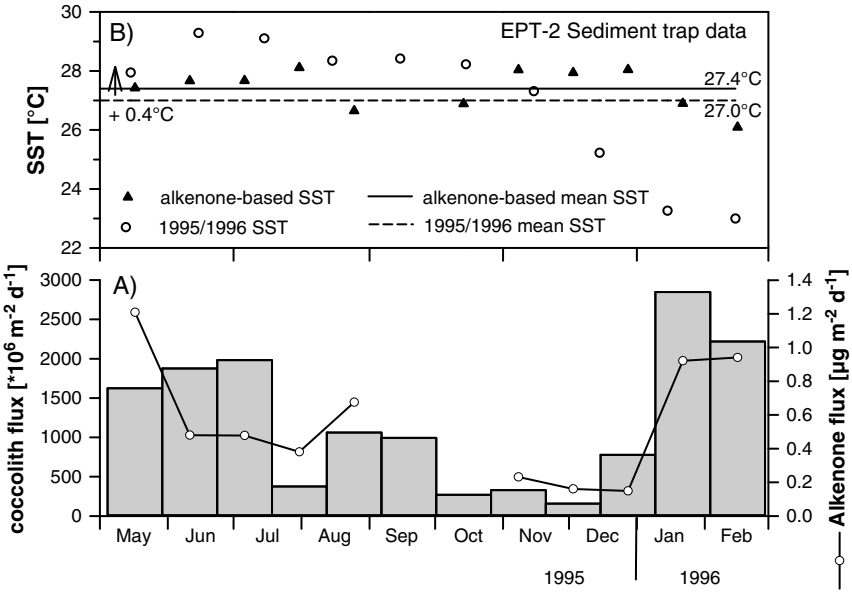

Figure 3. (a) Total coccolith (gray bars [*Andruleit et al.*, 2000]) and alkenone fluxes (open circles) at trap EPT-2 in the northeastern Arabian Sea off Pakistan. (b) Alkenone-derived SST measured in EPT-2 samples (triangle) compared to 1995/1996 monthly SST (circle; extracted from the website http://ingrid.ldgo.columbia.edu). Mean alkenone-based SST is about 0.4°C higher than mean temperature over May 1995 to February 1996.

alkenone (C_{37}, C_{38}, and C_{39}) fluxes in the central Arabian Sea [*Prahl et al.*, 2000]. Sediment trap studies from different parts of the Arabian Sea thus showed a strong coupling between coccolithophore (and alkenone) production and the seasonal cycle in this area [*Andruleit et al.*, 2000; *Broerse et al.*, 2000; *Prahl et al.*, 2000; *Wakeham et al.*, 2002].

This seasonality may bias the SST signal in sediments toward seasonal flux maxima, so that it may not be representative of the annual mean SST (AM-SST). In our set of trap samples covering the period from May 1995 to February 1996, the seasonal variability of alkenone-derived SST (26.1°C to 28.1°C; $U^{K'}_{37}$ from 0.904 to 0.971; Figure 3b) is attenuated compared to observed SSTs which vary from 23.0°C to 29.2°C [*Reynolds et al.*, 2002]. The observed mismatch between alkenone-based SST in sediment trap samples and regional seasonal SST patterns seems to be a general phenomenon independent on oceanic region (central Arabian Sea [*Prahl et al.*, 2000]; Sea of Okhotsk, northwest Pacific [*Seki et al.*, 2007], subtropical oligotrophic North Pacific [*Prahl et al.*, 2005]). In general, these studies found that alkenone-based SST produces a warm SST bias in winter and a cold SST bias in summer concordant with our observations from the northeastern Arabian Sea, where monthly average alkenone-based SSTs deviate most from modern observed SSTs during the cold winter months of the trapping period in 1995/1996. The overestimation of winter SST by alkenones may be explained by a change in the coccolithophore community to alkenone-producing species that exhibit a different response to growth temperature, thus altering the relationship of $U^{K'}_{37}$ ratio to SST [*Prahl et al.*, 2005]. At the Pakistan Margin, changes in the coccolithophore assemblage (including the alkenone-producing species *Emiliania huxleyi* and *Gephyrocapsa oceanica*) are mainly controlled by variations in the mean mixed layer depth and total nutrient availability [*Andruleit et al.*, 2004]. A change in the alkenone-producing coccolithophore community due to mixed layer deepening at site EPT-2 is well reflected in the ratio of *G. oceanica* to *E. huxleyi* that show an increasing abundance of *G. oceanica* relative *to E. huxleyi* in winter (see Figure S2 in the supporting information; coccolithore flux data were taken from *Andruleit et al.* [2000]). Although relative species composition of the two alkenone-producing coccolithophorides seems to be stable in the Indian Ocean sedimentary record (spatially [*Sonzogni et al.*, 1997a] as well as through time [*Doose-Rolinski et al.*, 2001]), we suggest that it might be of importance for $U^{K'}_{37}$ calibration on a seasonal scale on the Pakistan continental margin. If we use a linear offset of 0.085 (instead of 0.043) to calibrate the $U^{K'}_{37}$ index to SST as suggested by *Prahl et al.* [2005] for the deeply mixed wintertime, alkenone-based SST were much closer to observed SST at 10 m water depth (Figure S2 in the supporting information).

©2014. American Geophysical Union. All Rights Reserved.

On the other hand, the slight cold bias of alkenone-based SST in our trap samples during summer is best explained by alkenone production in the upper mixed layer between 0 to 30 m water depths.

Albeit the complexity of processes that plays a role in seasonal alkenone-based SST estimates, we state that sedimentary $U^{K'}_{37}$ measurements on the Pakistan Margin are best approximated by AM-SST. The average alkenone-derived SST of the sampling period is 27.4°C, which (considering an uncertainty of 0.5°C) matches well with the mean modern SST (27.0°C; see Figure 3b), which in turn is very close to the average mean SST from May to February obtained from the Levitus climatology (26.9°C [*Levitus and Boyer*, 1994]). Climatological annual mean SST (including the months missing in the trap investigation) is 26.4°C [*Levitus and Boyer*, 1994]. But because alkenones reflect an integrated signal of the upper 0 to 50 m of the water column [*Sonzogni et al.*, 1997a], small deviations from actual sea surface temperature measurements are to be expected.

Our interpretation of sedimentary $U^{K'}_{37}$ measurements as an AM-SST signal is supported by $U^{K'}_{37}$ estimates for sediment trap samples from the central Arabian Sea [*Prahl et al.*, 2000] and by a compilation of sediment trap time series distributed over different oceanic regions worldwide [*Rosell-Melé and Prahl*, 2013]. Furthermore, measurements of sediment core tops, which were used to develop an alkenone calibration equation for the Indian Ocean, showed no significant differences between calculated production-weighted temperature and AM-SST [*Sonzogni et al.*, 1997a, 1997b]. According to *Doose-Rolinski et al.* [2001], alkenone-derived SSTs measured in a Holocene section of a sediment core from the Pakistan Margin were best approximated by annual mean temperature as well.

4.2. Alkenone SST Record in Core 39KG/275KL

Alkenone SST vary between 26.9°C and 28.4°C ($U^{K'}_{37}$ from 0.932 to 0.981) over the last 2400 years and thus lie well above the modern annual mean of 26.4°C [*Levitus and Boyer*, 1994]. *Conte et al.* [2006] stated that a positive offset of reconstructed core top temperature (27.6°C for SO90-39KG) compared to atlas temperature is observed in several areas worldwide. It is alternatively explained by diagenetic alteration of alkenone ratios in the water column and/or surficial sediments, by lateral advection, or by variations in the seasonality and depth of alkenone production. In our view, diagenesis can be ruled out as a significant process affecting our $U^{K'}_{37}$ estimates, because the offset was also observed between trap alkenone SST and modern AM-SST and was furthermore confirmed by Mg/Ca temperatures [*Dahl and Oppo*, 2006]. Biasing of the alkenone signal by alkenones produced and advected from the upwelling area off Oman may be a factor [*Andruleit et al.,* 2000], but coccolithophore fluxes on the Pakistan Margin are only slightly enhanced during the SW monsoon season, and the associated bias in the alkenone signal must be of minor importance. As SSTs in the southeastern Arabian Sea remain relatively high during winter, lateral advection of water masses and alkenones from the southwest Indian coast (following the counterclockwise surface current established during the NE monsoon) on the other hand would result in a warm bias of alkenone SST on the Pakistan Margin during the winter. However, based on a comparison of coccolith fluxes with coccosphere fluxes (which should present a vertical flux signal), *Andruleit et al.* [2000] suggested that coccolithophore assemblages were not influenced by resuspension processes during this time of the year.

Regardless of the absolute SST, Figure 5 illustrates relative SST variations around the overall mean of 27.7°C over the last 2 millennia. Although the amplitude of the alkenone-derived SST signal is small in our record, our SST reconstruction exhibits statistical significant periods of long-term SST changes (see also detailed discussion of signal-to-noise ratio in the supporting information). SSTs were high at around 28.2°C until 250 A.D., rapidly decreased and outlined a time period of low SST that lasted from 400 to 1000 A.D. After a rebound to $>$28°C between 1000 and 1300 A.D., the decline in SST continued until minimum temperatures (26.9°C) are registered during the 18th century. The minimum of our SST reconstruction at this time agrees with the results obtained from a global climate proxy network, which suggests 0.3°C cooler SSTs than present during the Little Ice Age in the northeastern Arabian Sea [*Mann et al.*, 2009]. Our SST estimates, after this minimum, suggest a northern Arabian Sea warming tendency that persists to the present.

4.3. Records of Productivity

Our analytical approach to trace the past productivity changes were based on TOC concentrations, $\delta^{15}N$ values, and the ratio of carbonate to opal. The range of TOC concentrations (1.0 and 2.0%) and $\delta^{15}N$ values (7.1 to 8.5‰) in the sediment cores at sites 39KG/275KL (Figure 4) is a characteristic of high-productivity

©2014. American Geophysical Union. All Rights Reserved.

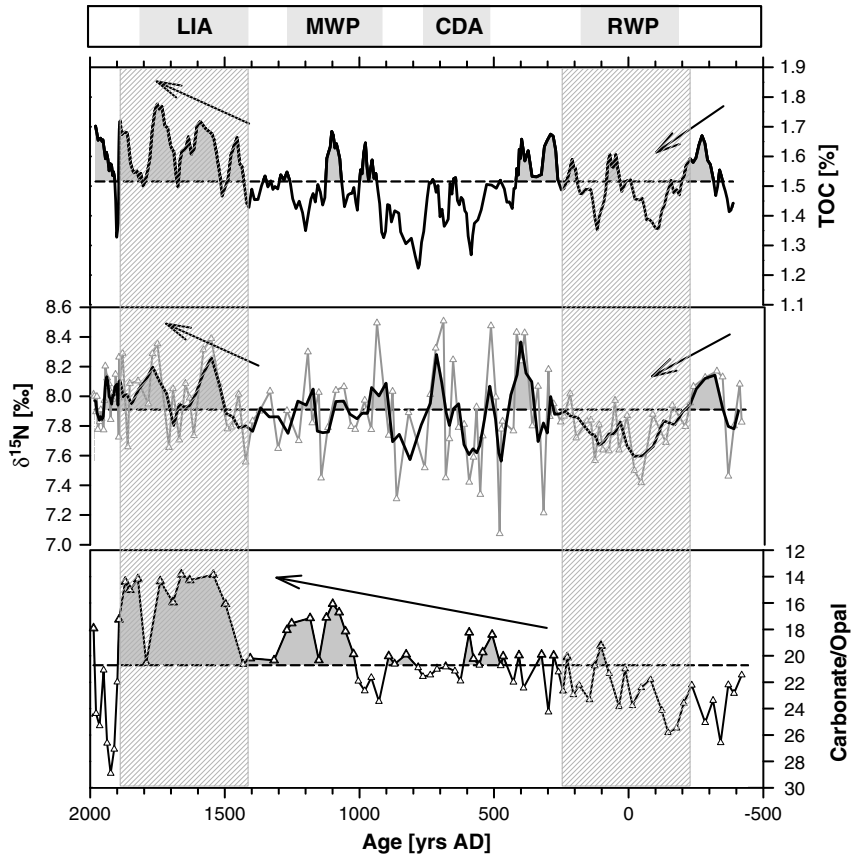

Figure 4. Late Holocene productivity record for cores 39KG and 275KL from the northeastern Arabian Sea. Carbonate/opal ratios, $\delta^{15}N$ values (bold line: running mean of 3) and smoothed TOC contents (running average of 5) were used as productivity indicators. The gray shaded areas indicate good agreement between productivity proxies. The dashed lines indicate the respective mean over the complete data set. Further illustrated are the characteristic climate periods known from the Northern Hemisphere: Little Ice Age (LIA), Medieval Warm Period (MWP), Cold Dark Ages (CDA), and Roman Warm Period (RWP).

areas with a well-developed OMZ and water column denitrification [e.g., *Naqvi et al.*, 1998; *Altabet et al.*, 1999; *Gaye-Haake et al.*, 2005] such as the northern Arabian Sea [*Cowie et al.*, 1999]. Organic carbon concentrations in sediments on the Pakistan Margin (and elsewhere) are influenced by surface productivity but also by dilution with lithogenic material, bottom water oxygen concentrations, bulk accumulation rate, sediment texture, refractory of organic matter, and the mineral surface area [e.g., *Paropkari et al.*, 1992; *Keil and Cowie*, 1999; *van der Weijden et al.*, 1999; *Suthhof et al.*, 2000].

At our core site, the use of organic carbon mass accumulation rates (TOC MAR) as a productivity indicator that theoretically remove an influence of dilution is complicated by strongly fluctuating sedimentation rates (SR) (ranging from 87 to 212 cm kyr^{-1}). Sediment mass accumulation rates (71 to 203 g cm^{-2} kyr^{-1}; event deposits excluded) calculated from SR and bulk densities are even higher than glacial/interglacial variations reported from the western (SR ranging from 6 to 38 cm kyr^{-1} and MAR ranging from 5 to 50 g cm^{-2} kyr^{-1} [*Emeis et al.*, 1995]) and eastern Arabian Sea (SR ranging from 4 to 9 cm kyr^{-1} [*Rostek et al.*, 1997]). SR and MAR at our study site are caused by highly variable input of lithogenic matter (range from 81 to 86%) from river runoff and/or dust storms [*Schulz et al.*, 1996; *von Rad et al.*, 1999]. Even though sedimentary OM in our core mainly consists of marine OM ($\delta^{13}C$ measured in core 275KL ranges from −21.5 to −19.5‰), significant positive correlations between TOC MAR and SR ($R^2 = 0.56$) and TOC MAR and sedimentary mass accumulation rates ($R^2 = 0.76$) indicate a dominant influence of bulk MAR (and thus alternating input of organic matter transported with mineral matter on its passage across the shelf) on organic carbon accumulation rates [*Müller and Suess*, 1979; *Emeis et al.*, 1995]. This conclusion is supported by the good agreement between

©2014. American Geophysical Union. All Rights Reserved.

downcore variations in TOC MAR and varve thickness, which is an indicator for precipitation and river runoff [*von Rad et al.*, 1999; see Figure S3 in the supporting information]. Thus, we infer that in our study area, TOC contents can be used as a tracer for the past primary productivity changes rather than the organic carbon accumulation rates. Although measured TOC contents during the period 400 to 900 A.D. might partly be affected by dilution as indicated by visual comparison of organic carbon concentrations with MAR (Figure S4 in the supporting information), no significant correlation between TOC contents and mass accumulation rates ($R^2 = 0.008$) could be observed indicating no significant control of the dilution on downcore variations in TOC concentrations.

Over the last 2400 years of our record, elevated TOC concentrations coincide with increased δ^{15}N values and vice versa, a relationship described for Holocene sediments [*Agnihotri et al.*, 2003] and over glacial/interglacial cycles [*Altabet et al.*, 1995; *Ganeshram et al.*, 2000; *Suthhof et al.*, 2001] in the northern Indian Ocean. Parallel changes in TOC concentrations and δ^{15}N are both related to the productivity variations caused by variable access to the subthermocline nitrate pool. That nitrate pool has a high δ^{15}N resulting from denitrification within the upper part of the OMZ [*Gaye et al.*, 2013]. Upwelling does not occur at our core location, so that variable deepening of the mixed layer due to convective winter mixing during the NE monsoon season is the most likely process transporting the ^{15}N-enriched nitrate to the ocean surface and enabling productivity. Together, δ^{15}N values and TOC concentrations in our sediment cores thus reflect productivity changes associated with mixed layer deepening due to NE monsoon conditions. A third indirect signal of productivity is the ratio of the biogenic constituents carbonate (ranging from 6 to 15.5%) and opal (ranging from 0.5 to 0.9%), because high nutrient availability induces diatom blooms and high flux rates or organic matter, whereas high carbonate rain rates indicate low nutrient availability. The carbonate to opal ratio ranges from 14 to 29 and indicates a dominance of carbonate primary producers (coccolithophores) at our study site that decreases over time relative to opal from diatoms [*Ramaswamy and Gaye*, 2006]. In this general trend, declining carbonate to opal ratios indicate a shift to higher productivity around 1400 A.D. (Figure 4).

As discussed above, proxies indicative of productivity changes are influenced by a lot of processes. To minimize the effect of processes not related to productivity variations and to better filter out the signal caused by productivity changes, a productivity index (combining TOC, δ^{15}N, and carbonate/opal) was calculated. First, the range of values for all three parameters was standardized to values between 0 and 1, so that the respective productivity indicators were equally weighted and comparable to each other. The sum of the standardized values was calculated and again standardized to values between 0 (low productivity) and 1 (high productivity). High productivity from 1400 to 1950 A.D. and periods of decreased productivity from about 200 B.C. to 250 A.D., as recorded by all individual productivity parameters (Figure 4, indicated by the gray shaded areas), are well reflected by our productivity index (Figure 5, not reverse *y* axis). In addition, superimposed on short-term variability, the productivity index shows a gradual trend to increasing primary production in the northeastern Arabian Sea over the late Holocene.

4.4. Variability in Sr/Ca Ratios

The relationship between elevated Sr/Ca ratios and increased winter monsoon activity was first proposed for glacial/interglacial intervals by *Reichart et al.* [1998] and was later adapted for Holocene sediments by *Lückge et al.* [2001]. These authors proposed that elevated Sr/Ca ratios image variations in mixed layer depths. Because aragonite has a higher Sr content than calcite, variations in Sr/Ca track the depth interval of the aragonite compensation depth (ACD), and the deepening of the ACD and higher Sr/Ca ratios indicates intensified deep winter mixing due to elevated winter monsoon activity [*Reichart et al.*, 1998]. A different mechanism for changes in Sr/Ca on millennial time scales was proposed by *Böning and Bard* [2009], who attributed the variations in Sr/Ca in the northeastern Arabian Sea to changes in the formation of Antarctic Intermediate Waters. Today, Antarctic Intermediate Water in the Arabian Sea can only be traced up to 5°N [*You*, 1998], so that for the 2400 year record here, this long-term variability is most likely irrelevant.

The Sr/Ca ratio in the sediment cores vary between 0.023 and 0.032 at sites 39KG/275KL (Figure 5), which are in the range of previously measured values for Holocene sediments from the Makran area [*Lückge et al.*, 2001]. The increase in Sr/Ca ratios indicates a shift to winter monsoon conditions on the Pakistan Margin around 700 A.D.

©2014. American Geophysical Union. All Rights Reserved.

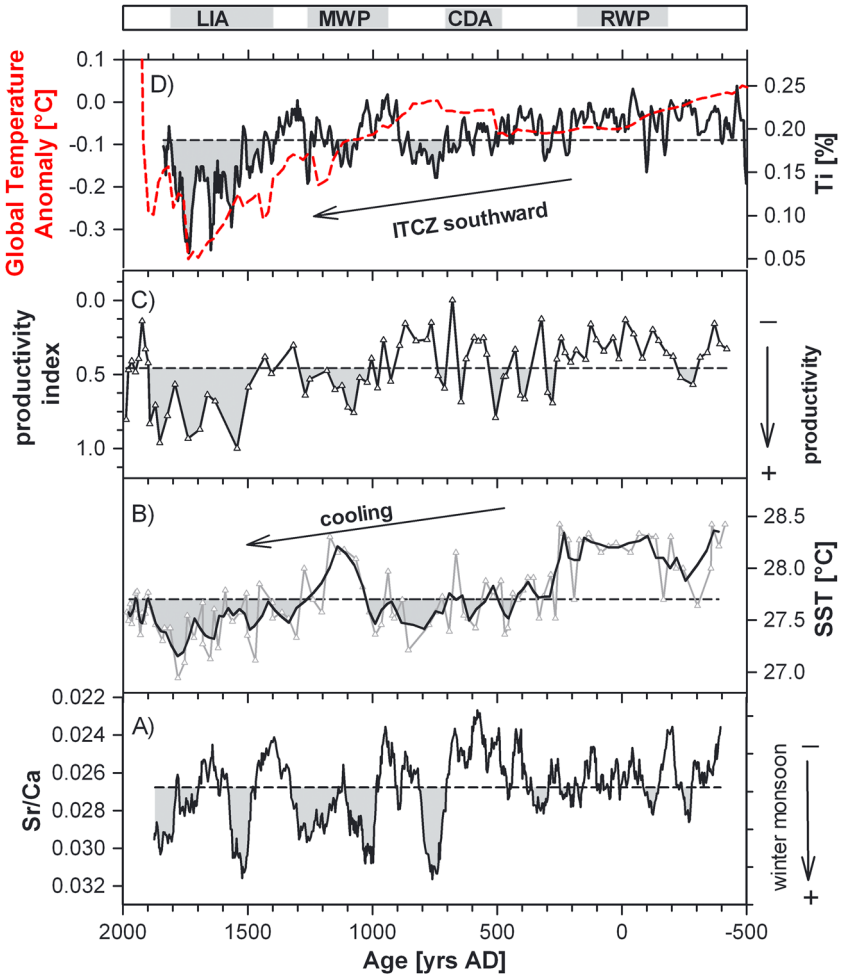

Figure 5. Reconstruction of winter monsoon variability in the northeastern Arabian Sea over the last 2400 years compared to long-term movements of the Intertropical Convergence Zone (ITCZ). (a) Smoothed Sr/Ca ratios (21 point running mean), (b) alkenone SST record (bold line: 3 point running mean), and (c) productivity index for core 39KG/275KL. (d) Titanium content of Cariaco Basin sediments as an indicator for the latitudinal shifts in the ITCZ [*Haug et al.*, 2001] compared to global temperature anomalies [*Marcott et al.*, 2013]. The dashed lines indicate the respective mean over the studied time interval.

5. Discussion

5.1. Productivity and SST Variability: Evidence for Monsoonal Change

Winter monsoon activity affects both sea surface temperature and mixed layer depth over the Pakistan Margin and thus controls the amount of thermocline nutrients entrained into the mixed layer (Figure 2). As a result, primary productivity changes in the northeastern Arabian Sea are strongly coupled to the intensity of the NE monsoon season. Whereas primary production is unambiguously related to monsoon strength, SST in the northeastern Arabian Sea, although primarily controlled by monsoon-related processes, can also be impacted by global temperature variations. A decrease in the alkenone-based SST signal at sites 39KG/275KL can thus be caused either by local strengthening of NE monsoon conditions or by globally lowered atmospheric temperature. If SST was changing as a response to varying NE monsoon intensity, then this should also be noted in our primary productivity reconstruction because intensified NE monsoon strength induces high rates of primary production at the Pakistan continental margin. The general trend of decreasing SST and increasing productivity seen in our record over the last 2400 years (Figure 5) confirms that alkenone SST primarily reflect changes in the NE monsoon strength. This coupling of SST and productivity is particularly pronounced during the periods from 400 B.C. to 300 A.D. and from 1400 A.D. until the present, while it is less clear between ~500 and 1300 A.D. Furthermore, alkenone SSTs follow the same

©2014. American Geophysical Union. All Rights Reserved.

pattern as reconstructed winter SSTs (based on planktic foraminifera transfer functions measured in the same sediment core; unpublished data) confirming the strong influence of the winter season on alkenone SST in this region.

A link between NE monsoon conditions, decreasing SSTs, and increasing productivity can be observed not only on a seasonal scale and over the last 2400 years but also on time scales of several hundreds of thousands of years. In the northeastern Arabian Sea, relatively high productivity and sea surface cooling appear to correspond to glacial stages due to elevated NE monsoon activity [e.g., *Rostek et al.*, 1997; *Schulte et al.*, 1999; *Schulte and Müller*, 2001].

5.2. Local Monsoon Dynamics in the Northeastern Arabian Sea During the Last 2400 Years

On the basis of the above-mentioned considerations, our multiproxy study from the northeastern Arabian Sea indicates three main periods of changing monsoon intensities throughout the late Holocene (Figure 5). Winter monsoon intensity was low before about 250 A.D. and is recorded by high SSTs and generally low primary production due to diminished northeasterly winds and reduced convective winter mixing in the northeastern Arabian Sea. Winter monsoon mixing strengthened after 250 A.D., which caused a cooling of the sea surface and slightly increased primary production. Finally, winter monsoon conditions started to predominate off Pakistan at about 700 A.D., as indicated by a shift to higher Sr/Ca ratios in core 275KL (Figure 5, note reverse Sr/Ca *y* axis). Weak correlation between SST and primary productivity from ~500 to 1300 A.D. suggests a "transition period" from weak to strengthening NE monsoon, characterized by unstable and fluctuating environmental conditions on the Pakistan Margin. Strong winter monsoon activity prevailed during the Little Ice Age (LIA) from 1400 to 1900 A.D., as indicated by low SSTs and a peak in biological productivity due to strong convective winter mixing. Low SSTs during the LIA as well as relatively high SSTs due to diminished NE monsoon conditions occurring 2000 years ago agree with another northeastern Arabian Sea (alkenone-based) SST reconstruction [*Doose-Rolinski et al.*, 2001]. Although both SST records differ in detail, possibly as a result of proxy uncertainty, they display similar trends of warming at around 0 A.D. and cooling during the LIA. This small-scale variability between both records might further be caused by the analysis of different core sections and thus variations in the time interval which is integrated by the alkenones.

The dynamics of the monsoon low-level wind system on the Pakistan Margin throughout the last 2400 years affect marine processes as well as moisture changes in this area. Variable but relatively low-salinity values after 500 A.D. probably reflect diminished SW monsoon and/or enhanced NE monsoon conditions [*Doose-Rolinski et al.*, 2001]. *Lückge et al.* [2001] proposed a shift from SW monsoon-dominated precipitation to NE monsoon precipitation in the Makran area around 500 A.D. These findings match our interpretation of predominating NE monsoon conditions since ~700 A.D.

Enhanced NE monsoonal activity during the LIA was most likely induced by an increased influence of westerlies in the Makran area during this period. Today, winter rainfall brought by westerly winds and connected to cyclonic storms originating in the Mediterranean significantly contributes to the total annual precipitation in the study area [*Lückge et al.*, 2001; *von Rad et al.*, 2002b, and references therein]. Higher precipitation implicating stronger westerlies on the coast off Pakistan after 1600 A.D. and during the LIA was deduced from varve thickness data from the nearby cores SO90/56KA [*von Rad et al.,* 1999] and in a cave record from the central Kumaun Himalaya [*Sanwal et al.*, 2013]. A significant feature preceding the LIA in the northeastern Arabian Sea is a distinct phase of increased SST (1050 to 1300 A.D.; see Figure 5) that coincides with the Medieval Warm Period (MWP), a time of generally warm climate conditions observed in the Northern Hemisphere.

The response of the marine system to regional monsoon dynamics is best explained by the reactions of the surface ocean to seasonal shifts in the ITCZ. The reversal of low-level winds in the Arabian Sea during the seasonal cycle is accompanied by a shift in the location of the ITCZ. Core sites 39KG/275KL are located at the average northern latitudinal position of the ITCZ, and thus, surface ocean processes in this area are sensitive to the long-term movements of the annual mean position of the ITCZ and the associate change in prevailing low-level winds. Northward migration of the ITCZ in spring (SW monsoon) and southward retreat in autumn (NE monsoon) differentially impact on surface ocean salinity and temperature and thus thermocline depth in the northeastern Arabian Sea. At times when the northern position of the ITCZ slightly shifts south of the average position, the duration of NE monsoon influence at site 275KL during winter is prolonged. This would enhance the influence of the winter monsoon on surface ocean conditions in this area.

©2014. American Geophysical Union. All Rights Reserved.

Different studies widely distributed over the low-latitude region [e.g., *Haug et al.*, 2001; *Fleitmann et al.*, 2007; *Russell and Johnson*, 2005] indicate a general southward shift of the annual mean position of the ITCZ over the late Holocene in response to global climate variability. We argue that long-term southward movement of the ITCZ throughout the late Holocene is responsible for the long-term trends of declining sea surface temperature and rising productivity seen in our record (Figure 5). In this long-term trend, times of the southernmost ITCZ displacements were contemporaneous with the periods of highest primary productivity and lowest SST on the Pakistan continental margin. Both reflect an increasing regional influence of the NE monsoon and a reaction of the surface ocean by progressive winter deepening of convective mixing. This argument is supported by *Jung et al.* [2004], who attributed coherent basin-wide decadal to century-scale temperature variations in the Arabian Sea during the Holocene (based on a correlation between SST variations off Somalia and Pakistan) to a shift in the mean position of the ITCZ throughout the Holocene. Such a connection between a southward migrating annual mean position of the ITCZ and monsoon as well as precipitation changes throughout the Holocene was proposed by several authors [*Haug et al.*, 2001; *Lückge et al.*, 2001; *Fleitmann et al.*, 2003, 2007; *Russell and Johnson*, 2005; *Wang et al.*, 2005; *Yancheva et al.*, 2007; *Sinha et al.*, 2011].

5.3. Reversed Behavior Between Summer and Winter Monsoon Strength During the Late Holocene

The mechanism above argues for an inverse relationship between summer and winter monsoon strength throughout the Indian and East Asian monsoon domain in the time-variant location of the ITCZ, expressed by the decreasing summer monsoon intensity with increasing winter monsoon activity and vice versa [e.g., *Reichart et al.*, 2002; *Yancheva et al.*, 2007]. Is this inverse relationship evident in a comparison of our winter monsoon record with records of summer monsoon strength? The regions influenced most drastically by the SW monsoon are the Oman and the Somalia upwelling systems, that both registered a gradual warming of sea surface temperatures during the last 2400 years [*Huguet et al.*, 2006], in contrast to decreasing SST on the Pakistan Margin over this period. This points to a general antagonistic behavior in the millennial trend of summer and winter monsoon strength over the late Holocene. However, summer and winter monsoon were more variable on centennial time scales, particularly during the time intervals of greatest climate contrast over the last 2000 years on the Northern Hemisphere, namely, the MWP (950 to 1250 A.D.) and the LIA (1400 to 1800 A.D.). Evidence for increased summer monsoon intensity during the MWP comes from the northwestern Arabian Sea [*Anderson et al.*, 2002, 2010; *Gupta et al.*, 2003], from Oman [*Fleitmann et al.*, 2004], India [*Sinha et al.*, 2007, 2011], as well as from China [*Zhang et al.*, 2008]. Changes in winter monsoon strength off Pakistan during this time are less pronounced. While higher SST argues for diminished NE monsoon activity over the northeastern Arabian Sea, slightly enhanced primary production and relatively higher Sr/Ca ratios might be indicative of NE monsoon intensification. One possible explanation for this mismatch might be that primary productivity on the Pakistan Margin during this time is fueled by lateral advection of nutrients from the upwelling area off Oman due to intensified summer monsoon circulation. On the other hand, most studies reconstructed diminished SW monsoon strength during the LIA [*Fleitmann et al.*, 2004; *Sinha et al.*, 2011; *Zhang et al.*, 2008], when our record suggests increased NE monsoon activity over the Pakistan Margin.

During the last 400 years, however, SW monsoon strengthens again in the northwestern Arabian Sea, probably as a result of a general warming trend [*Anderson et al.*, 2002]. Speleothem $\delta^{18}O$ from Kahf Defore in southern Oman indicates summer monsoon rainfall generally above the long-term average since 1660 A.D. and supports this hypothesis [*Fleitmann et al.*, 2004]. However, in the Pakistan Margin record, winter monsoon indicators continue to dominate over the last 400 years. Only most recently (since 1900 A.D.), primary productivity on the Pakistan Margin appears to decrease and SSTs increase slightly, suggestive of diminished NE monsoon conditions in the northeastern Arabian Sea. The Oman cave record on land may be more sensitive to summer monsoon changes than the marine record in the Makran area, which is dominated by winter monsoon variability.

The antagonism of SW and NE monsoon is evidenced by the comparison of our winter monsoon record with other monsoon reconstructions in the Arabian Sea and beyond. Based on the assumption that the $\delta^{18}O$ signal measured in speleothems from Wanxiang Cave is mainly influenced by summer monsoon precipitation, *Zhang et al.* [2008] compiled a 1810 year long record of summer monsoon intensity for central China. Their $\delta^{18}O$ variations show a strong resemblance to our reconstructed SST curve with lower SST in the

©2014. American Geophysical Union. All Rights Reserved.

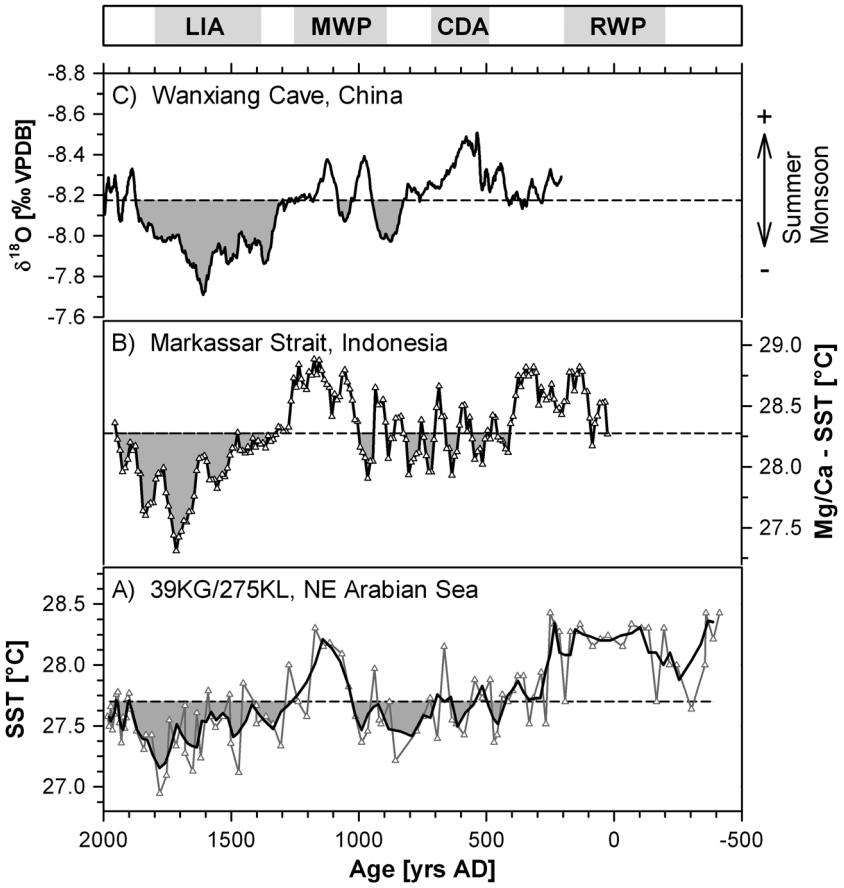

Figure 6. (a) Late Holocene alkenone-derived SST variations (cores 39KG and 275KL) from the northeastern Arabian Sea compared to (b) Mg/Ca-SST variations reconstructed for the Markassar Strait (Indonesia) by *Oppo et al.* [2009] and (c) a smoothed $\delta^{18}O$ record (15 point moving average) of Wanxiang Cave (China) as an indicator for the summer monsoon intensity from *Zhang et al.* [2008]. The dashed lines indicate the respective mean over the studied time interval.

northeastern Arabian Sea, coinciding with a decline in summer monsoon rainfall in central China due to weaker East Asian summer monsoon intensity (Figure 6). Furthermore, SST variations in the northeastern Arabian Sea are not only related to changes in East Asian summer monsoon over central China but also to changes in SSTs from the Indo-Pacific warm pool [*Oppo et al.*, 2009, Figure 6]. In accordance with our interpretation, *Oppo et al.* [2009] suggested that strong sea surface cooling in the Markassar Strait during the LIA was caused by intensified winter monsoon conditions rather than by monsoon-induced upwelling. We thus conclude that a linkage between summer and winter monsoon strength exists over the whole Asian monsoon system during the late Holocene, reflecting long-term and short-term shifts in the ITCZ.

5.4. Global Connections: The LIA Climate Feature

The monsoon record from the Pakistan Margin is in phase with characteristic, northern hemispheric climate periods of the late Holocene, such as the Little Ice Age, the Medieval Warm Period, and the Roman Warm Period (RWP). It reveals a consistent pattern of diminished winter monsoon activity in the northeastern Arabian Sea during northern hemispheric warm periods (MWP and RWP) and strengthened winter monsoon activity during hemispheric colder periods (LIA). Our high-resolution record implies that this consistent link between the North Atlantic and the Indian Ocean, which was described for glacial/interglacial [e.g., *Sirocko et al.*, 1993; *Schulz et al.*, 1998; *Schulte and Müller*, 2001] to climatological [*Gupta et al.*, 2003] time scales, appears to operate during historical times as well. It causes the SW monsoon to weaken and the NE monsoon to gain strength during colder climate conditions over the North Atlantic.

One of the most prominent climate features in the northeastern Arabian Sea over the last 2400 years was the sharp decrease in SST due to the strengthening NE monsoon conditions between 1400 and 1850 A.D.,

©2014. American Geophysical Union. All Rights Reserved.

contemporaneous with the LIA. Once described as a climate period restricted only to the northern extratropical hemisphere [e.g., *Keigwin*, 1996], LIA climate conditions appear to have impacted on SST in low-latitude regions as well [*DeMenocal*, 2000; *Black et al.*, 2007; *Oppo et al.*, 2009]. A recently published global data set of proxy records indeed confirms a global cooling trend between 1580 and 1880 A.D. [*PAGES 2k Consortium*, 2013] that is preceded by a phase of low solar irradiance between 1450 and 1750 A.D. [*Bard et al.*, 2000], suggesting that LIA climate conditions may at least partly be influenced by solar forcing. Solar radiation has been proposed as a forcing mechanism controlling both North Atlantic climate [*Bond et al.*, 2001] as well as variations in monsoon intensity during the Holocene [*Neff et al.*, 2001; *Agnihotri et al.*, 2002; *Fleitmann et al.*, 2003; *Gupta et al.*, 2005; *Wang et al.*, 2005]. We thus infer that the decline in SST and increased NE monsoonal wind strength in the northeastern Arabian Sea during the LIA were triggered by global colder climate conditions (as a response to radiative forcing such as solar output, aerosols, and greenhouse gases), accompanied by southward displacement of the ITCZ.

6. Conclusions

Our high-resolution reconstruction of primary productivity and alkenone-derived SST from the northeastern Arabian Sea provides a unique record of winter monsoon variability throughout the late Holocene. In this area, primary production and sea surface temperatures are linked to winter monsoon intensity that cools the sea surface and increases its salinity so that thermocline deepening entrains more nutrients into the mixed layer and raises productivity. Because core 275KL is located in a sensitive region at the modern northern mean latitudinal position of the ITCZ, observed changes in surface ocean properties in response to the monsoonal wind regime on the Pakistan Margin track long-term and short-term movements of the ITCZ throughout the late Holocene. Reconstructed SST decreased whereas productivity increased over the last 2400 years, imaging a long-term trend of NE monsoon strengthening in response to insolation-induced southward migration of the ITCZ. Comparison of our winter monsoon record with records of summer monsoon intensity confirms an antagonistic relationship between summer and winter monsoon strength during the last 2400 years.

Reconstructed monsoon variability supports the growing body of evidence that significant climate variability occurs not only on time scales of several hundred of thousand years but also through the late Holocene. Before 250 A.D., winter monsoon activity in the northeastern Arabian Sea was generally weak, and convective winter mixing was shallow, indicated by high SSTs (~28.3°C) and reduced primary productivity. Winter monsoon conditions started to predominate off Pakistan at about 700 A.D., in response to the overall southward movement of average ITCZ location during the late Holocene. While winter monsoon activity was relatively unstable from ~500 to 1300 A.D., strong sea surface cooling down to 26.9°C and a peak in primary productivity indicated strong and prevailing winter monsoon activity during the LIA from 1400 to 1900 A.D. The coherence between monsoon-induced variations over the Pakistan Margin with other monsoon records indicates a strong linkage of climate variability in the entire Asian monsoon system during the late Holocene, caused by migration of the ITCZ.

Acknowledgments
We thank S. Beckmann and F. Langenberg for their analytical support. Financial support was provided by the German Federal Ministry of Education and Research (BMBF) grant 03G0806B (CARIMA) and is gratefully acknowledged. This is a NIO contribution. Data will be available at www.pangaea.de.

References

Agnihotri, R., K. Dutta, R. Bhushan, and B. L. K. Somayajulu (2002), Evidence for solar forcing on the Indian monsoon during the last millennium, *Earth Planet. Sci. Lett.*, *198*, 521–527.

Agnihotri, R., S. K. Bhattacharya, M. M. Sarin, and B. L. K. Somayajulu (2003), Changes in surface productivity and subsurface denitrification during the Holocene: A multiproxy study from the eastern Arabian Sea, *The Holocene*, *13*, 701–713, doi:10.1191/0959683603hl656rp.

Agnihotri, R., S. Kurian, M. Fernandes, K. Reshma, W. D'Souza, and S. W. A. Naqvi (2008), Variability of subsurface denitrification and surface productivity in the coastal eastern Arabian Sea over the past seven centuries, *The Holocene*, *18*, 755–764, doi:10.1177/0959683608091795.

Altabet, A., D. W. Murray, and W. L. Prell (1999), Climatically linked oscillation in Arabian Sea denitrification over the past 1 m.y.: Implications for the marine N cycle, *Paleoceanography*, *14*, 732–743, doi:10.1029/1999PA900035.

Altabet, M. A., R. Francois, D. W. Murray, and W. L. Prell (1995), Climate-related variations in denitrification in the Arabian Sea from sediment $^{15}N/^{14}N$ ratios, *Nature*, *373*, 506–509.

Anderson, D. M., J. T. Overpeck, and A. K. Gupta (2002), Increase in the Asian Southwest Monsoon during the past Four Centuries, *Science*, *297*(5581), 596–599.

Anderson, D. M., C. K. Baulcomb, A. K. Duvivier, and A. K. Gupta (2010), Indian summer monsoon during the last two millennia, *J. Quat. Sci.*, *25*, 911–917, doi:10.1002/jqs.1369.

Andruleit, H. A., U. von Rad, A. Bruns, and V. Ittekkot (2000), Coccolithophore fluxes from sediment traps in the northeastern Arabian Sea off Pakistan, *Mar. Micropaleontol.*, *38*, 285–308.

Andruleit, H., U. Rogalla, and S. Stäger (2004), From living communities to fossil assemblages: Origin and fate of coccolithophores in the northern Arabian Sea, *Micropaleontology*, *50*, 5–21.

©2014. American Geophysical Union. All Rights Reserved.

Banse, K., and C. R. McClain (1986), Winter blooms of phytoplankton in the Arabian Sea as observed by the Coastal Zone Color Scanner, *Mar. Ecol. Prog. Ser.*, *34*, 201–211.
Bard, E., G. Raisbeck, F. Yiou, and J. Jouzel (2000), Solar irradiance during the last 1200 years based on cosmogenic nuclides, *Tellus*, *52B*(3), 985–992, doi:10.1034/j.1600-0889.2000.d01-7.x.
Berkelhammer, M., A. Sinha, M. Mudelsee, H. Cheng, R. L. Edwards, and K. G. Cannariato (2010), Persistent multidecadal power of the Indian Summer Monsoon, *Earth Planet. Sci. Lett.*, *290*, 166–172, doi:10.1016/j.epsl.2009.12.017.
Black, D. E., M. A. Abahazi, R. C. Thunell, A. Kaplan, E. J. Tappa, and L. C. Peterson (2007), An 8-century tropical Atlantic SST record from the Cariaco Basin: Baseline variability, twentieth-century warming, and Atlantic hurricane frequency, *Paleoceanography*, *22*, PA4204, doi:10.1029/2007PA001427.
Bond, G., B. Kromer, J. Beer, R. Muscheler, M. N. Evans, W. Showers, S. Hoffmann, R. Lotti-Bond, I. Hajdas, and G. Bonani (2001), Persistent Solar Influence on North Atlantic Climate During the Holocene, *Science*, *294*, 2130–2136, doi:10.1126/science.1065680.
Böning, P., and E. Bard (2009), Millennial/centennial-scale thermocline ventilation changes in the Indian Ocean as reflected by aragonite preservation and geochemical variations in Arabian Sea sediments, *Geochim. Cosmochim. Acta*, *73*, 6771–6788, doi:10.1016/j.gca.2009.08.028.
Broerse, A. T. C., G.-J. A. Brummer, and J. E. Van Hinte (2000), Coccolithophore export production in response to monsoonal upwelling off Somalia (northwestern Indian Ocean), *Deep Sea Res., II*, *47*, 2179–2205, doi:10.1016/S0967-0645(00)00021-7.
Burns, S. J., D. Fleitmann, M. Mudelsee, U. Neff, A. Matter, and A. Mangini (2002), A 780-year annually resolved record of Indian Ocean monsoon precipitation from a speleothem from south Oman, *J. Geophys. Res.*, *107*(D20), 4434, doi:10.1029/2001JD001281.
Chauhan, O. S., E. Vogelsang, N. Basavaiah, and U. S. A. Kader (2010), Reconstruction of the variability of the southwest monsoon during the past 3 ka, from the continental margin of the southeastern Arabian Sea, *J. Quat. Sci.*, *25*(5), 798–807.
Clemens, S., W. L. Prell, D. W. Murray, G. Shimmield, and G. Weedon (1991), Forcing mechanisms of the Indian Ocean monsoon, *Nature*, *353*, 720–725.
Conley, D. J. (1998), An interlaboratory comparison for the measurement of biogenic silica in sediments, *Mar. Chem.*, *63*, 39–48, doi:10.1016/S0304-4203(98)00049-8.
Conte, M. H., M.-A. Sicre, C. Rühlemann, J. C. Weber, S. Schulte, D. Schulz-Bull, and T. Blanz (2006), Global temperature calibration of the alkenone unsaturation index ($U^{K'}_{37}$) in surface waters and comparison with surface sediments, *Geochem. Geophys. Geosyst.*, *7*, Q02005, doi:10.1029/2005GC001054.
Cowie, G. L., S. E. Calvert, T. F. Pedersen, H. Schulz, and U. von Rad (1999), Organic content and preservational controls in surficial shelf and slope sediments from the Arabian Sea (Pakistan margin), *Mar. Geol.*, *161*, 23–38.
Dahl, K. A., and D. W. Oppo (2006), Sea surface temperature pattern reconstructions in the Arabian Sea, *Paleoceanography*, *21*, PA1014, doi:10.1029/2005PA001162.
DeMaster, D. J. (1981), The supply and accumulation of silica in the marine environment, *Geochim. Cosmochim. Acta*, *45*, 1715–1732, doi:10.1016/0016-7037(81)90006-5.
DeMenocal, P. (2000), Coherent High- and Low-Latitude Climate Variability During the Holocene Warm Period, *Science*, *288*, 2198–2202, doi:10.1126/science.288.5474.2198.
Doose-Rolinski, H., U. Rogalla, G. Scheeder, A. Lückge, and U. von Rad (2001), High-resolution temperature and evaporation changes during the late Holocene in the northeastern Arabian Sea, *Paleoceanography*, *16*, 358–367, doi:10.1029/2000PA000511.
Emeis, K.-C., D. M. Anderson, H. Doose-Rolinski, D. Kroon, and D. Schulz-Bull (1995), Sea-Surface Temperatures and the History of Monsoon Upwelling in the Northwest Arabian Sea during the Last 500,000 Years, *Quat. Rese.*, *43*, 355–361.
Fleitmann, D., S. J. Burns, M. Mudelsee, U. Neff, J. Kramers, A. Mangini, and A. Matter (2003), Holocene forcing of Indian Monsoon recorded in a Stalagmite from Southern Oman, *Science*, *300*(5626), 1737–1739.
Fleitmann, D., S. J. Burns, U. Neff, M. Mudelsee, A. Mangini, and A. Matter (2004), Palaeoclimatic interpretation of high-resolution oxygen isotope profiles derived from annually laminated speleothems from Southern Oman, *Quat. Sci. Rev.*, *23*, 935–945.
Fleitmann, D., et al. (2007), Holocene ITCZ and Indian monsoon dynamics recorded in stalagmites from Oman and Yemen (Socotra), *Quat. Sci. Rev.*, *26*, 170–188, doi:10.1016/j.quascirev.2006.04.012.
Ganeshram, S., F. Pedersen, E. Calvert, W. McNeill, and M. R. Fontugne (2000), Glacial-interglacial variability in denitrification in the world's oceans: Causes and consequences, *Paleoceanography*, *15*, 361–376, doi:10.1029/1999PA000422.
Gaye, B., B. Nagel, K. Dähnke, T. Rixen, and K.-C. Emeis (2013), Evidence of parallel denitrification and nitrite oxidation in the ODZ of the Arabian Sea from paired stable isotopes of nitrate and nitrite, *Global Biogeochem. Cycles*, *27*, 1059–1071, doi:10.1002/2011GB004115.
Gaye-Haake, B., et al. (2005), Stable nitrogen isotopic ratios of sinking particles and sediments from the northern Indian Ocean, *Mar. Chem.*, *96*, 243–255, doi:10.1016/j.marchem.2005.02.001.
Gupta, A. K., D. M. Anderson, and J. T. Overpeck (2003), Abrupt changes in the Asian southwest monsoon during the Holocene and their links to the North Atlantic Ocean, *Nature*, *421*, 354–356.
Gupta, A. K., M. Das, and D. M. Anderson (2005), Solar influence on the Indian summer monsoon during the Holocene, *Geophys. Res. Lett.*, *32*, L17703, doi:10.1029/2005GL022685.
Gupta, A. K., K. Mohan, S. Sarkar, S. C. Clemens, R. Ravindra, and R. K. Uttam (2011), East–West similarities and differences in the surface and deep northern Arabian Sea records during the past 21 Kyr, *Palaeogeogr. Palaeoclimatol. Palaeoecol.*, *301*, 75–85, doi:10.1016/j.palaeo.2010.12.027.
Haake, B., V. Ittekkot, T. Rixen, V. Ramaswamy, R. R. Nair, and W. B. Curry (1993), Seasonality and interannual variability of particle fluxes to the deep Arabian Sea, *Deep Sea Res., I*, *40*(7), 1323–1344.
Hastenrath, S., and P. J. Lamb (1979), *Climate Atlas of the Indian Ocean, Surface Climate and Atmospheric Circulation*, vol. 1, Univ. of Wisconsin Press, Madison.
Haug, G. H., K. A. Hughen, D. M. Sigman, L. C. Peterson, and U. Röhl (2001), Southward migration of the intertropical convergence zone through the Holocene, *Science*, *293*, 1304–1308, doi:10.1126/science.1059725.
Huguet, C., J.-H. Kim, J. S. Sinninghe Damsté, and S. Schouten (2006), Reconstruction of sea surface temperature variations in the Arabian Sea over the last 23 kyr using organic proxies (TEX_{86} and $U^{K'}_{37}$), *Paleoceanography*, *21*, PA3003, doi:10.1029/2005PA001215.
Jung, S. J. A., G. R. Davies, G. Ganssen, and D. Kroon (2004), Synchronous Holocene sea surface temperature and rainfall variations in the Asian monsoon system, *Quat. Sci. Rev.*, *23*, 2207–2218.
Keigwin, L. D. (1996), The Little Ice Age and Medieval Warm Period in the Sargasso Sea, *Science*, *274*, 1504–1508.
Keil, R. G., and G. L. Cowie (1999), Organic matter preservation through the oxygen-deficient zone of the NE Arabian Sea as discerned by organic carbon: Mineral surface area ratios, *Mar. Geol.*, *161*, 13–22, doi:10.1016/S0025-3227(99)00052-3.
Levitus, S., and T. Boyer (1994), *World Ocean Atlas 1994, Temperature, NOAA Atlas NESDIS*, vol. 4, U.S. department of Commerce, Washington, D. C.

©2014. American Geophysical Union. All Rights Reserved.

Lückge, A., H. Doose-Rolinski, A. A. Khan, H. Schulz, and U. von Rad (2001), Monsoonal variability in the northeastern Arabian Sea during the past 5000 years: Geochemical evidence from laminated sediments, *Palaeogeogr. Palaeoclimatol. Palaeoecol.*, *167*, 273–286.

Lückge, A., L. Reinhardt, H. Andruleit, H. Doose-Rolinski, U. von Rad, H. Schulz, and U. Treppke (2002), Formation of varve-like laminae off Pakistan: Decoding 5 years of sedimentation, *Geol. Soc. London Spec. Publ.*, *195*, 421–431.

Madhupratap, M., S. Prasanna Kumar, P. M. A. Bhattathiri, M. Dileep Kumar, S. Raghukumar, K. K. C. Nair, and N. Ramaiah (1996), Mechanism of the biological response to winter cooling in the northeastern Arabian Sea, *Nature*, *384*, 549–552.

Mann, M. E., Z. Zhang, S. Rutherford, R. S. Bradley, M. K. Hughes, D. Shindell, C. Ammann, G. Faluvegi, and F. Ni (2009), Global Signatures and Dynamical Origins of the Little Ice Age and Medieval Climate Anomaly, *Science*, *326*, 1256–1260, doi:10.1126/science.1177303.

Marcott, S. A., J. D. Shakun, P. U. Clark, and A. C. Mix (2013), A Reconstruction of Regional and Global Temperature for the Past 11,300 Years, *Science*, *339*, 1198–1201, doi:10.1126/science.1228026.

Müller, P. J., and E. Suess (1979), Productivity, sedimentation rate, and sedimentary organic matter in the oceans-I. Organic carbon preservation, *Deep Sea Res.*, *26A*, 1347–1362.

Nair, R. R., V. Ittekkot, S. J. Manganini, V. Ramaswamy, B. Haake, E. T. Degens, B. N. Desai, and S. Honjo (1989), Increased particle flux to the deep ocean related to monsoons, *Nature*, *338*, 749–751.

Naqvi, S. W. A., T. Yoshinari, D. A. Jayakumar, M. A. Altabet, P. V. Narvekar, A. H. Devol, J. A. Brandes, and L. A. Codispoti (1998), Budgetary and biogeochemical implications of N_2O isotope signatures in the Arabian Sea, *Nature*, *394*, 462–464.

Neff, U., S. J. Burns, A. Mangini, M. Mudelsee, D. Fleitmann, and A. Matter (2001), Strong coherence between solar variability and the monsoon in Oman between 9 and 6 kyr ago, *Nature*, *411*, 290–293, doi:10.1038/35077048.

Olson, D. B., G. L. Hitchcock, R. A. Fine, and B. A. Warren (1993), Maintenance of the low-oxygen layer in the central Arabian Sea, *Deep Sea Res., II*, *40*(3), 673–685.

Oppo, D. W., Y. Rosenthal, and B. K. Linsley (2009), 2,000-year-long temperature and hydrology reconstructions from the Indo-Pacific warm pool, *Nature*, *460*, 1113–1116, doi:10.1038/nature08233.

PAGES 2k Consortium (2013), Continental-scale temperature variability during the past two millennia, *Nat. Geosci.*, *6*, 339–346, doi:10.1038/NGEO1797.

Paropkari, A. L., C. P. Babu, and A. Mascarenhas (1992), A critical evaluation of depositional parameters controlling the variability of organic carbon in Arabian Sea sediments, *Mar. Geol.*, *107*, 213–226.

Prahl, F. G., J. Dymond, and M. A. Sparrow (2000), Annual biomarker record for export production in the central Arabian Sea, *Deep Sea Res., Part II*, *47*, 1581–1604, doi:10.1016/S0967-0645(99)00155-1.

Prahl, F. G., B. N. Popp, D. M. Karl, and M. A. Sparrow (2005), Ecology and biogeochemistry of alkenone production at Station ALOHA, *Deep Sea Res., Part I*, *52*, 699–719, doi:10.1016/j.dsr.2004.12.001.

Prasanna Kumar, S., and T. G. Prasad (1996), Winter cooling in the northern Arabian Sea, *Curr. Sci.*, *71*(10), 834–841.

Prasanna Kumar, S., N. Ramaiah, M. Gauns, V. V. S. S. Sarma, P. M. Muraleedharan, S. Raghukumar, M. Dileep Kumar, and M. Madhupratap (2001), Physical forcing of biological productivity in the Northern Arabian Sea during the Northeast Monsoon, *Deep Sea Res., Part II*, *48*, 1115–1126, doi:10.1016/S0967-0645(00)00133-8.

Ramaswamy, V., and B. Gaye (2006), Regional variations in the fluxes of foraminifera carbonate, coccolithophorid carbonate and biogenic opal in the northern Indian Ocean, *Deep Sea Res., I*, *53*, 271–293, doi:10.1016/j.dsr.2005.11.003.

Reichart, G. J., L. J. Lourens, and W. J. Zachariasse (1998), Temporal variability in the northern Arabian Sea Oxygen Minimum Zone (OMZ) during the last 225,000 years, *Paleoceanography*, *13*, 607–621, doi:10.1029/98PA02203.

Reichart, G. J., S. J. Schenau, G. J. de Lange, and W. J. Zachariasse (2002), Synchroneity of oxygen minimum zone intensity on the Oman and Pakistan Margins at sub-Milankovitch time scales, *Mar. Geol.*, *185*, 403–415, doi:10.1016/S0025-3227(02)00184-6.

Reynolds, R. W., N. A. Rayner, T. M. Smith, D. C. Stokes, and W. Wang (2002), An Improved In Situ and Satellite SST Analysis for Climate, *J. Clim.*, *15*, 1609–1625.

Rixen, T., B. Haake, V. Ittekkot, M. V. S. Guptha, R. R. Nair, and P. Schlüssel (1996), Coupling between SW monsoon-related surface and deep ocean processes as discerned from continuous particle flux measurements and correlated satellite data, *J. Geophys. Res.*, *101*, 569–582.

Rixen, T., M. V. S. Guptha, and V. Ittekkot (2005), Deep ocean fluxes and their link to surface ocean processes and the biological pump, *Prog. Oceanogr.*, *65*, 240–259, doi:10.1016/j.pocean.2005.03.006.

Rosell-Melé, A., and F. G. Prahl (2013), Seasonality of $U^{K'}_{37}$ temperature estimates as inferred from sediment trap data, *Quat. Sci. Rev.*, *72*, 128–136, doi:10.1016/j.quascirev.2013.04.017.

Rostek, F., E. Bard, L. Beaufort, C. Sonzogni, and G. Ganssen (1997), Sea surface temperature and productivity records for the past 240 kyr in the Arabian Sea, *Deep Sea Res., II*, *44*(6–7), 1461–1480.

Russell, J. M., and T. C. Johnson (2005), Late Holocene climate change in the North Atlantic and equatorial Africa: Millennial-scale ITCZ migration, *Geophys. Res. Lett.*, *32*, L17705, doi:10.1029/2005GL023295.

Sanwal, J., B. S. Kotlia, C. Rajendran, S. M. Ahmad, K. Rajendran, and M. Sandiford (2013), Climatic variability in Central Indian Himalaya during the last 1800 years: Evidence from a high resolution speleothem record, *Quat. Int.*, doi:10.1016/j.quaint.2013.03.029.

Schlitzer, R. (2013), Ocean Data View. [Available at http://odv.awi-bremerhaven.de.]

Schulte, S., and P. Müller (2001), Variations of sea surface temperature and primary productivity during Heinrich and Dansgaard-Oeschger events in the northeastern Arabian Sea, *Geo-Mar. Lett.*, *21*, 168–175, doi:10.1007/s003670100080.

Schulte, S., F. Rostek, E. Bard, J. Rullkötter, and O. Marchal (1999), Variations of oxygen-minimum and primary productivity recorded in sediments of the Arabian Sea, *Earth Planet. Sci. Lett.*, *173*, 205–221, doi:10.1016/S0012-821X(99)00232-0.

Schulz, H., U. von Rad, and U. Von Stackelberg (1996), Laminated sediments from the oxygen-minimum zone of the northeastern Arabian Sea, *Geol. Soc. London Spec. Publ.*, *116*, 185–207, doi:10.1144/GSL.SP.1996.116.01.16.

Schulz, H., U. von Rad, and H. Erlenkeuser (1998), Correlation between Arabian Sea and Greenland climate oscillations of the past 110,000 years, *Nature*, *393*, 54–57.

Schulz, H., U. von Rad, and V. Ittekkot (2002), Planktic foraminifera, particle flux and oceanic productivity off Pakistan, NE Arabian Sea: Modern analogues and application to the palaeoclimatic record, *Geol. Soc. London Spec. Publ.*, *195*, 499–516, doi:10.1144/GSL.SP.2002.195.01.27.

Seki, O., T. Nakatsuka, K. Kawamura, S.-I. Saitoh, and M. Wakatsuchi (2007), Time-series sediment trap record of alkenones from the western Sea of Okhotsk, *Mar. Chem.*, *104*, 253–265, doi:10.1016/j.marchem.2006.12.002.

Sinha, A., K. G. Cannariato, L. D. Stott, H. Cheng, R. L. Edwards, M. G. Yadava, R. Ramesh, and I. B. Singh (2007), A 900-year (600 to 1500 A.D.) record of the Indian summer monsoon precipitation from the core monsoon zone of India, *Geophys. Res. Lett.*, *34*, L16707, doi:10.1029/2007GL030431.

©2014. American Geophysical Union. All Rights Reserved.

Sinha, A., L. D. Stott, M. Berkelhammer, H. Cheng, R. L. Edwards, B. Buckley, M. Aldenderfer, and M. Mudelsee (2011), A global context of megadroughts in monsoon Asia during the past millennium, *Quat. Sci. Rev.*, *30*, 47–62.

Sirocko, F., M. Sarnthein, H. Erlenkeuser, H. Lange, M. Arnold, and J. C. Duplessy (1993), Century-scale events in monsoonal climate over the past 24,000 years, *Nature*, *364*, 322–324.

Sonzogni, C., E. Bard, F. Rostek, R. Lafont, A. Rosell-Mele, and G. Eglinton (1997a), Core-top calibrations of the alkenone index vs sea surface temperature in the Indian Ocean, *Deep Sea Res., II*, *44*(6–7), 1445–1460.

Sonzogni, C., E. Bard, F. Rostek, D. Dollfus, A. Rosell-Melé, and G. Eglinton (1997b), Temperature and Salinity Effects on Alkenone Ratios Measured in Surface Sediments from the Indian Ocean, *Quat. Res.*, *47*, 344–355.

Suthhof, A., T. C. Jennerjahn, P. Schäfer, and V. Ittekkot (2000), Nature of organic matter in surface sediments from the Pakistan continental margin and the deep Arabian Sea: Amino acids, *Deep Sea Res., II*, *47*, 329–351.

Suthhof, A., V. Ittekkot, and B. Gaye-Haake (2001), Millennial-scale oscillation of denitrification intensity in the Arabian Sea during the late Quaternary and its potential influence on atmospheric N_2O and global climate, *Global Biogeochem. Cycles*, *15*, 637–649, doi:10.1029/2000GB001337.

van der Weijden, C. H., G. J. Reichart, and H. J. Visser (1999), Enhanced preservation of organic matter in sediments deposited within the oxygen minimum zone in the northeastern Arabian Sea, *Deep Sea Res., I*, *46*, 807–830, doi:10.1016/S0967-0637(98)00093-4.

Van Rampelbergh, M., et al. (2013), Mid- to late Holocene Indian Ocean Monsoon variability recorded in four speleothems from Socotra Island, Yemen, *Quat. Sci. Rev.*, *65*, 129–142, doi:10.1016/j.quascirev.2013.01.016.

von Rad, U., H. Schulz, and SONNE 90 Scientific Party (1995), Sampling the oxygen minimum zone off Pakistan: Glacial-interglacial variations of anoxia and productivity (preliminary results, SONNE 90 cruise), *Mar. Geol.*, *125*, 7–19.

von Rad, U., M. Schaaf, K. H. Michels, H. Schulz, W. H. Berger, and F. Sirocko (1999), A 5000-yr Record of Climate Change in Varved Sediments from the Oxygen Minimum Zone off Pakistan, Northeastern Arabian Sea, *Quat. Res.*, *51*, 39–53.

von Rad, U., G. Delisle, and A. Lückge (2002a), Comment - On the formation of laminated sediments on the continental margin off Pakistan, *Mar. Geol.*, *192*, 425–429.

von Rad, U., A. A. Khan, W. H. Berger, D. Rammlmair, and U. Treppke (2002b), Varves, turbidites and cycles in upper Holocene sediments (Makran slope, northern Arabian Sea), *Geol. Soc. London Spec. Publ.*, *195*, 387–406.

Wakeham, S. G., M. L. Peterson, J. I. Hedges, and C. Lee (2002), Lipid biomarker fluxes in the Arabian Sea, with a comparison to the equatorial Pacific Ocean, *Deep Sea Res., II*, *49*, 2265–2301, doi:10.1016/S0967-0645(02)00037-1.

Wang, Y., H. Cheng, R. L. Edwards, Y. He, X. Kong, Z. An, J. Wu, M. J. Kelly, C. A. Dykoski, and X. Li (2005), The Holocene Asian Monsoon: Links to Solar Changes and North Atlantic Climate, *Science*, *308*, 854–857, doi:10.1126/science.1106296.

Wyrtki, K. (1973), Physical Oceanography of the Indian Ocean, in *The Biology of the Indian Ocean*, edited by B. Zeitzschel, pp. 18–36, Springer, Berlin.

Yancheva, G., N. R. Nowaczyk, J. Mingram, P. Dulski, G. Schettler, J. F. W. Negendank, J. Liu, D. M. Sigman, L. C. Peterson, and G. H. Haug (2007), Influence of the intertropical convergence zone on the East Asian monsoon, *Nature*, *445*, 74–77, doi:10.1038/nature05431.

You, Y. (1998), Intermediate water circulation and ventilation of the Indian Ocean derived from water-mass contributions, *J. Mar. Res.*, *56*, 1029–1067, doi:10.1357/002224098765173455.

Zhang, P., et al. (2008), A Test of Climate, Sun, and Culture Relationships from an 1810-Year Chinese Cave Record, *Science*, *322*, 940–942.

©2014. American Geophysical Union. All Rights Reserved.